# SUPPLEMENTARY MATERIAL: Influence of volume shrinkage and axial force variation on the rheological characterization of waxy oils

André da Silva Guimarães[1,2], Thiago Oliveira Marinho[3†], Pedro Tavares Pereira[1†], Príamo Albuquerque Melo[1†], Roney Leon Thompson[4†], Marcio Nele[1*†]

[1*]Programa de Engenharia Química (PEQ/COPPE), Universidade Federal do Rio de Janeiro, Avenida Horácio Macedo -Bloco G, Rio de Janeiro, 21941-598, Rio de Janeiro, Brazil.
[2]Department of Chemical Engineering, Faculty of Natural Sciences, Norwegian University of Science and Technology, Sem Sælands vei, Trondheim, 7034, Trøndelag, Norway.
[3]EDIVIT Corporate Office, Petrobras, Av. Nossa Sra. da Penha, Vitória, 29057-550, Espírito Santo, Brazil.
[4]Programa de Engenharia Mecânica (PEM/COPPE), Universidade Federal do Rio de Janeiro, Avenida Horácio Macedo -Bloco G, Rio de Janeiro, 21941-598, Rio de Janeiro, Brazil.

*Corresponding author(s). E-mail(s): nele@eq.ufrj.br;
Contributing authors: asguimaraes@peq.coppe.ufrj.br; thiagomarinho333@gmail.com; pedro.pereira@peq.coppe.ufrj.br ; melo@peq.coppe.ufrj.br; rthompson@pem.coppe.ufrj.br;
†These authors contributed equally to this work.

# A Wax and oil composition assessment by Gas Chromatography (GC)

## A.1 Methodology

Gas chromatography (GC) tests with a mass spectrometer (MSD) and a flame ionization detector (FID) were performed to assess the sample composition. The tests were conducted on an Agilent 7890B instrument. The chromatograph was equipped with a 7693A injector, a 5977B MSD detector, and a capillary column DB-1HT with a 30 m length, 0.25 mm diameter, 0.1 $\mu$m film thickness, and helium as the carrier gas. The protocols based on Ruwoldt et al. [1] and Savasdipol et al. [2] are described as follows.

For the wax, the column temperature program was defined as follows: 100 °C for 5 min; 100 °C to 300 °C at 5 °C·min$^{-1}$; and 10 min at 300 °C. In addition, the inlet temperature was set at 320 °C. During the procedure, 0.3 $\mu L$ of sample was injected in splitless mode. For the MSD detector, the quad, transfer line, and source temperatures were set to 150, 230, and 300 °C, respectively. A 7-minute delay and a detection range of 42 to 600 g·mol$^{-1}$ were also defined. The helium initial flow rate was set to 1 mL·min$^{-1}$, and the post-run flow rate to 1.2 mL·min$^{-1}$. For the FID detector, the initial temperature was 100 °C.

Since the oil has lighter components than wax, the column temperature program was altered to start at 75 °C. Furthermore, a heating rate of 1.5 °C·min$^{-1}$ was defined at the interval of 75 to 125 °C. The MSD detector's time delay was also altered to 5 min. All wax and oil tests were conducted in duplicate.

For sample preparation, the wax was diluted in hexane (Sigma-Aldrich, ≥ 95%) to 0.1 wt%. Octacosane (C28) from Sigma-Aldrich (99 % purity) and tetracosane (C24) from Alfa Aesar (99 % purity) were used as references. The C24 and C28 samples were diluted in hexane at a concentration m/v of 40 ppm each. The oil was also diluted in hexane at 0.05 v/v% [2].

## A.2 Results

The total ion chromatogram (TIC) and the FID signal from mineral oil and paraffin wax are shown in Figures 1 and 2, respectively.

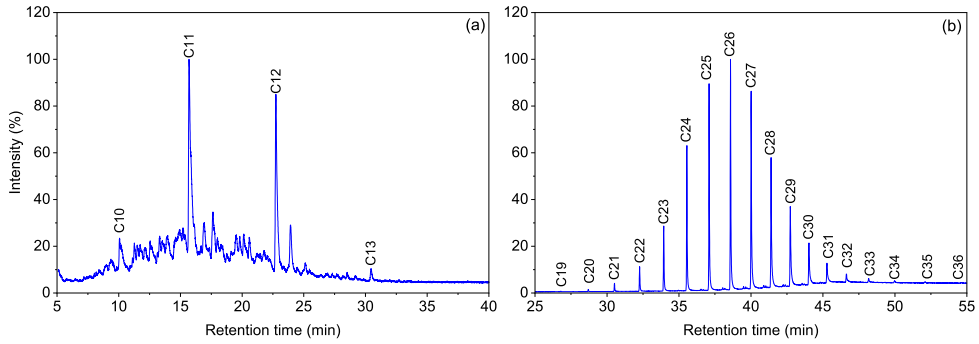


**Fig. 1** Total ion chromatogram for the Exxsol D60 mineral oil (a) and SASOL 5405 paraffin wax (b).

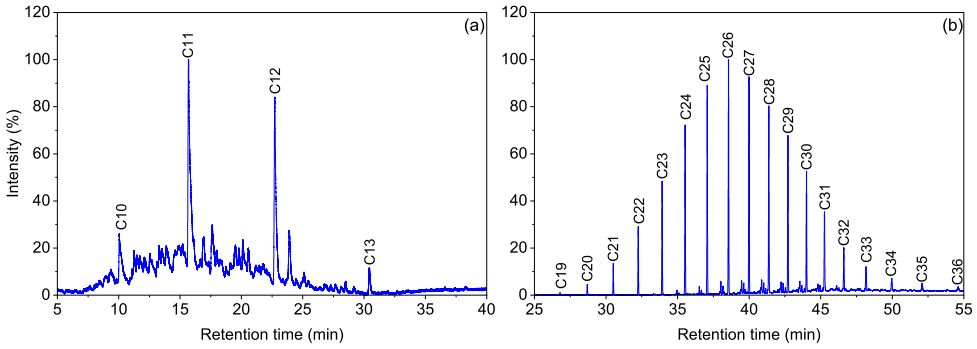


**Fig. 2** FID chromatogram for Exxsol D60 mineral oil (a) and SASOL 5405 paraffin wax (b).

# B Wax and oil thermal characterization

## B.1 Methodology

DSC tests were conducted on a Q2000 differential scanning calorimeter (TA Instruments, USA) to characterize the material's thermal behavior. The experiments were performed using Tzero aluminum hermetic pans with a sample weight of about 15 mg.

For the wax, the thermal protocol consisted of equilibrating the sample at 80 °C and cooling at 0.5, 1, and 2 °C·min$^{-1}$ to -40 °C. At -40 °C, after the sample had equilibrated, it was heated to the initial temperature at the same cooling rate. The same protocol was repeated for the oil, starting from 50 °C.

## B.2 Results

Table 1 lists the crystallization and melting enthalpies and temperatures for the wax.

**Table 1** Transition temperatures and enthalpies for the wax.

| Cooling rate (°C/min) | Crystallization temperature (°C) | Melting temperature (°C) | Crystallization enthalpy (J/g) | Melting enthalpy (J/g) |
|---|---|---|---|---|
| 0.5 | 54.4 ± 0.1 | 55.8 ± 0.2 | 197.1 ± 2.4 | 177.8 ± 2.9 |
| 1 | 54.6 ± 0.1 | 56.1 ± 0.2 | 196.1 ± 2.4 | 178.6 ± 2.9 |
| 2 | 54.5 ± 0.1 | 56.8 ± 0.2 | 196.7 ± 2.4 | 178.7 ± 2.9 |

The thermograms obtained are shown in Figure 3 for wax (a) and mineral oil (b). Mineral oil showed no thermal events over the investigated temperature range.

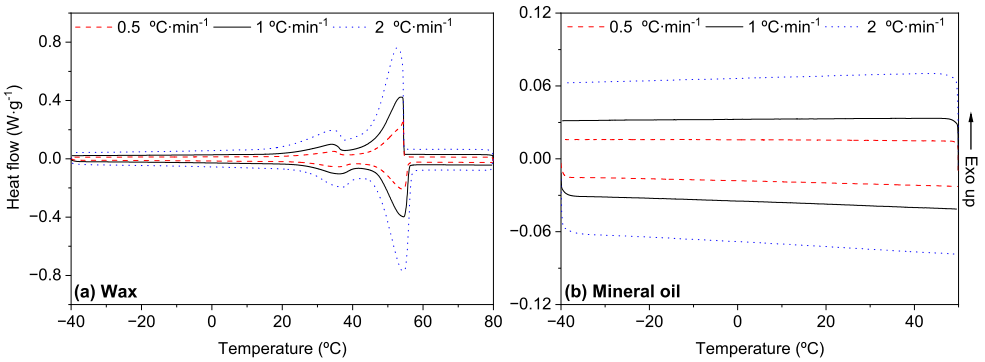


**Fig. 3** (a) Wax and (b) mineral oil thermograms.

# C Mineral oil rheology

## C.1 Methodology

The mineral oil rheology was assessed using a shear rate sweep performed at 50 °C (0.01 to 1000 $s^{-1}$). The sweep was followed by cooling from 50 to 4 °C at 1.5 °C·$min^{-1}$, and the sample was sheared at 10 $s^{-1}$ to evaluate oil viscosity as a function of temperature. For this, a sandblasted cone-and-plate sensor with a 40 mm diameter, an angle of 2°, and a roughness of 6.25 $\mu$m was used. An upper-heated Peltier system model H-PTD200 was also coupled with the geometry.

The viscosity data as a function of temperature were fitted using the Andrade [3] model for the viscosity of liquids, as shown in Eq. 1:

$$\eta_0(T) = \eta_i \exp\left(\frac{E_\eta}{RT}\right) \tag{1}$$

in which, $\eta_i$ is the viscosity coefficient and $E_\eta/R$ represents the exponential constant. Moreover, $E_\eta/R$ can be interpreted as the ratio between the activation energy for viscous flow ($E_\eta$) and the universal gas constant ($R$). The temperature is provided in Kelvin.

The rheology data were evaluated based on the rheometer's minimum torque limit and the possibility of flow instability. In this regard, the methodology of Ewoldt et al. [4] was applied. Eq. 2 shows the expressions for the minimum readable viscosity ($\eta_{min}$). $F_\tau$ is the stress geometry factor, $M_{min,rot}$ represents the minimum torque of the equipment for rotation.

$$\eta_{min} = \frac{F_\tau M_{min,rot}}{\dot{\gamma}} \tag{2}$$

The criteria for flow instabilities for cone-plate geometry followed the Eq. 3, considering a critical Reynolds number of 4 [4],

$$\eta_{max} > \frac{\beta^3 R^2 \rho \dot{\gamma}}{4} \tag{3}$$

where $\beta$ is the cone angle, $R$ is the geometry radius, $\rho$ is the material density, and $\eta_{max}$ is the maximum viscosity value. Beyond $\eta_{max}$, it is assumed that secondary flow occurrence is possible.

## C.2 Results

Figure 4 shows the oil flow curve at 50 °C for the cone-and-plate geometry. According to the flow curve in Figure 4, the oil behaves as a Newtonian fluid between the minimum torque and secondary flow limits. The average viscosity in this region is 0.84 ± 0.06 mPa·s. It is observed that the data fluctuate until approximately 7 $s^{-1}$, which corresponds to the minimum torque limit of the equipment of 0.1 $\mu$N·m. Concerning the secondary flow limit, no appreciable growth in viscosity was observed below 200 $s^{-1}$.

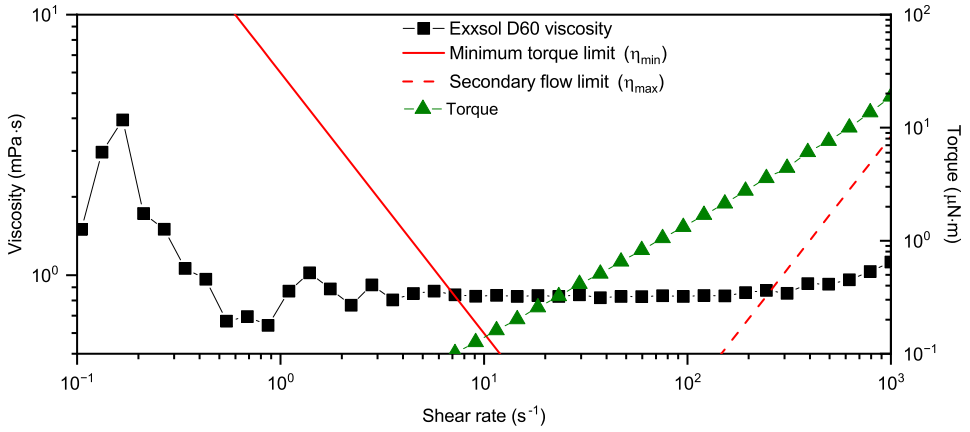


**Fig. 4** Exxsol D60 flow curve at 50 °C.

Figure 5 shows the viscosity behavior with temperature at 10 $s^{-1}$. The curve behavior in Figure 5 follows the Andrade [3] model for the viscosity of liquids with a determination coefficient of 0.97. The parameters of the model are also presented in the figure.

# D Cavity pictures

This section provides evidence of cavity formation in the studied waxymodel oil samples. Figure 6 shows the random pattern of cavities formed in 10 wt% samples at 4 °C, and Figure 7 shows the cavity formed at 4 °C in a 10 wt% sample and its effect on the gel in the cup (b) and on the bob (c) after geometry lift-up.

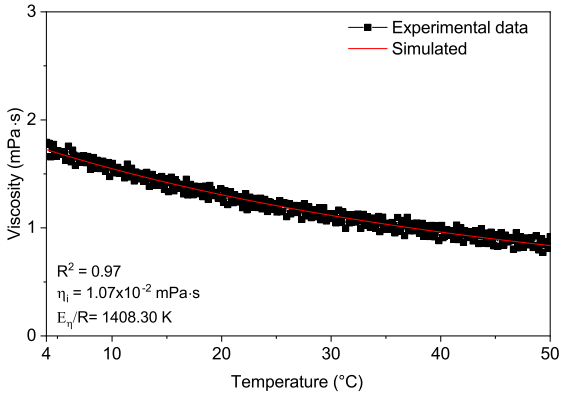


**Fig. 5** Exxsol D60 viscosity with temperature between 4 and 50 °C at 1.5 °C·min$^{-1}$: experimental and simulated.



**Fig. 6** Evidence of cavity formation on 10 wt% samples at 4 °C.

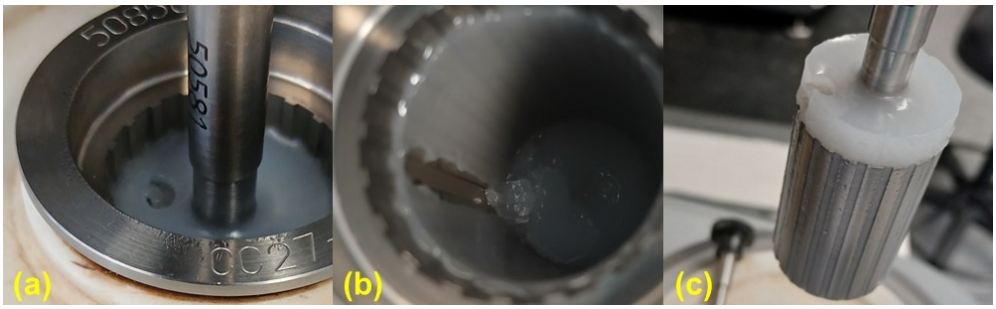


**Fig. 7** Representative example of cavity formation in a 10 wt% sample at 4 °C (a), and the effects of the cavity on the sample in the cup (b) and on the bob (c) after geometry lift-up.

# References


[1] Ruwoldt, J., Sørland, G.H., Simon, S., Oschmann, H.-J., Sjöblom, J.: Inhibitor-wax interactions and ppd effect on wax crystallization: New approaches for gc/ms and nmr, and comparison with dsc, cpm, and rheometry. Journal of Petroleum Science and Engineering **177**, 53–68 (2019)

[2] Savasdipol, A., Paradee, N., Niamlang, S.: The recovery process of used hydrocarbon solvent by vacuum distillation. In: IOP Conference Series: Materials Science and Engineering, vol. 559, p. 012018 (2019). IOP Publishing

[3] Andrade, E.d.C.: The viscosity of liquids. Nature **125**(3148), 309–310 (1930)

[4] Ewoldt, R.H., Johnston, M.T., Caretta, L.M.: Experimental challenges of shear rheology: How to avoid bad data. In: Spagnolie, S.E. (ed.) Complex Fluids in Biological Systems: Experiment, Theory, and Computation, pp. 207–241. Springer, New York (2015)